npj | Flexible Electronics

www.nature.com/npjflexelectron

ARTICLE OPEN

Check for updates

Flexible biodegradable transparent heaters based on fractal-like leaf skeletons

Vipul Sharma[1]✉, Anastasia Koivikko[1], Kyriacos Yiannacou[1], Kimmo Lahtonen[2] and Veikko Sariola[1]✉

We present a facile method to prepare flexible, transparent, biodegradable, and fast resistive heaters by applying silver (Ag) nanowires onto fractal-like leaf skeletons. The fractal-like structure of the leaf skeleton maximizes its surface area, improving the transfer of heat to its surroundings and thus making the heater fast, without compromising transparency. Ag ion layer on the leaf skeleton helps to conformally cover the surface with Ag nanowires. The sheet resistance of the heater can be controlled by the loading of Ag nanowires, without sacrificing the optical transmittance (~80% at 8 Ω sq^{-1}). The heating is uniform and the surface temperature of a 60 mm × 60 mm heater (8 Ω sq^{-1}) can quickly (5–10 s) raise to 125 °C with a low voltage (6 V). The heater displays excellent mechanical flexibility, showing no significant change in resistance and heating temperature when bent up to curvature of 800 m^{-1}. Finally, we demonstrate the potential of the bioinspired heater as a thermotherapy patch by encapsulating it in a biodegradable tape and mounting it on the human wrist and elbow. This study shows that fractal-like structures from nature can be repurposed as fractal designs for flexible electronics.

npj Flexible Electronics (2020)4:27 ; https://doi.org/10.1038/s41528-020-00091-8

INTRODUCTION

Transparent resistive film heaters have applications in defogging/defrosting[1], wearable devices[2], and industrial heat systems[3], among others[4–6]. In wearable devices, film heaters have been used in thermotherapy pads[7], sensors[8], thermochromic displays[9], and microfluidic chips[10]. In orthopedics, medical thermotherapy pads are commonly used to reduce pain, improve blood circulation, and decrease inflammation in human bodies[11]. These are also used in the treatment of various arthritis[12] (e.g., rheumatic arthritis and scapulohumeral peri arthritis), stiff joints, cervical spondylosis, and physical injuries[6,7,13].

The most common types of thermotherapy pads are based on a heating component and a far-infrared paste or gel[11]. The conventional thermotherapy pads have many drawbacks that limit their usage in wearable devices[11,14,15]. The first drawback is the lack of transparency, which is necessary to see the treatment effect without the need for removing the pads. Secondly, these are composed of mechanically stiff and planar parts that limit their flexibility. Thirdly, operation at low voltages is desirable for wearable devices[16]. Finally, the heating should be uniform and fast.

To be applicable in flexible electronic applications, the heaters must be flexible without plastic deformations. To make such heaters, engineered nanomaterials such as metal nanowires[17–19], carbon nanotubes[20], graphene[21], and other nanocomposites[4,22] have been proposed. In general, the film heaters are of different types such as metal oxide thin film-based heaters[23], carbon nanostructures-based heaters[9], metal nanowire network-based heaters[24,25], metal mesh[26], and hybrid electrodes-based heaters as reviewed in a work by Gupta et al.[4]. Among those, hybrid electrodes-based heaters make use of mesh-like architecture in combination with the conductive films[27]. These provide a synergistic approach for the design of efficient heaters operating on low power. In the recent reports, hybrid heaters composed of metal nanowires and woven fibers ranging from micrometers to nanometers have displayed good performances[17,28]. Many polymer-based elastomers[25], films[29], and fabrics[30] have also been used as flexible substrates to support metal nanowires for the fabrication of hybrid flexible and transparent heaters, especially for the thermotherapy applications. Owing to their mesh-like structure, sparse metal nanowire films display low sheet resistances and decent transmittance values. In these types of heaters, increasing the metal nanowire concentration is directly proportional to the decrease in sheet resistance. However, an increase in metal nanowire concentration leads to a drastic decrease in transmittance values[17]. The transmittance values can be controlled in these types of heaters if the mesh architecture is periodically woven. For instance, Hsu et al.[31] reported a hybrid transparent electrode composed of mesoscale copper wires and gold nanowires fabricated via the e-beam lithography process. The electrodes obtained displayed very low sheet resistance and high transmittance values. However, the fabrication process to create the periodic mesh at micro and nanoscale requires state of the art nanofabrication techniques and requires high cost. Apart from this, the patches thus obtained are limited to a few square millimeters and their scale-up is expensive and time-consuming. Apart from the good transmittance and low sheet resistance, thermal stability, structure design and mechanical properties of the substrates are also important in heaters meant to be used in flexible electronic applications[32].

The hierarchical architectures present in the natural materials can serve as guides to solve the restrictions of the materials and engineering techniques[33]. Recently, nature-inspired fractal-like structures have been integrated into engineering applications[34,35]. These applications include solar cells[35], antenna design[36], tissue engineering[37], optoelectronics[38], and heat transfer[39]. Mathematically, fractals are structures that appear similar at all length-scales and fractal-like structures can be found in nature in abundance. Different types of fractal-like structures can be seen in snowflakes and leaf venations, which range from the nanoscale to macroscale.

[1]Faculty of Medicine and Health Technology, Tampere University, Finland Korkeakoulunkatu 3, 33720 Tampere, Finland. [2]Faculty of Engineering and Natural Sciences, Tampere University, P.O. Box 692, 33014 Tampere, Finland. ✉email: vipul.sharma@tuni.fi; veikko.sariola@tuni.fi

Published in partnership with Nanjing Tech University

npj nature partner journals

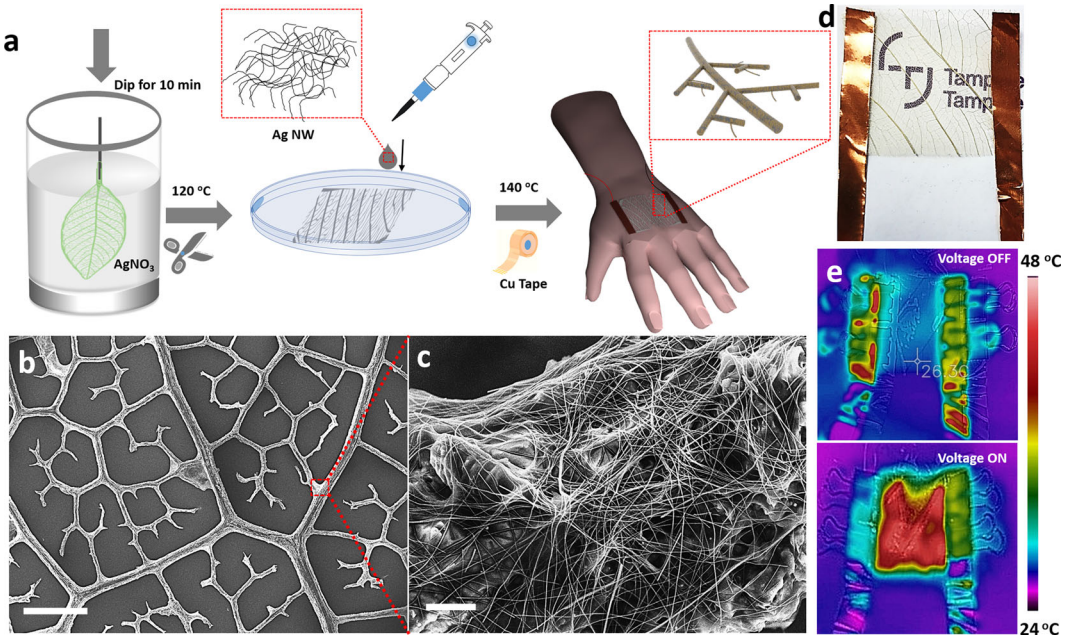

Fig. 1 Fabrication and general morphology. a Schematic of fabrication of a bioinspired thermotherapy patch. **b**, **c** SEM images of Ag nanowire-coated skeleton. **d** The final assembled bioinspired thermotherapy patch. **e** The infrared thermal camera images of the bioinspired thermotherapy patch. The scale bars in **b** and **c** are 500 and 10 μm, respectively.

These fractal-like structures can show almost perfect self-similarity, each repeating sub structure resembling the whole structure[40]. The fractal design is known to provide the optimal surface coverage, improved stability, efficient transport of ions[38]. The unique design also facilitates the efficient collection of electrical and thermal energy[41]. Han et al.[34] studied the quasi fractal structured electrodes for solar cell applications and reported that an increase in hierarchical orders of the fractal structures decreases the sheet resistances of electrodes significantly. However, in all the studies reporting the use of hierarchical fractal structures, expensive and complex fabrication techniques were used, which cannot be extended to a large scale.

Here, we report a bioinspired, highly flexible, and transparent heater based on the fractal-like leaf skeletons and Ag nanowires and demonstrate its use as a wearable thermotherapy patch. A simple fabrication method was used to conformally load the Ag nanowires on to the leaf skeleton that displays a multi-scale fractal-like structure. A seed layer of Ag ions is used to adhere to the Ag nanowires conformally to the surfaces. The presence of the seed layer increases junctions between the Ag nanowires and decreases the junction resistances. Sheet resistance is one of the most critical parameters of sheet-like heating elements[17]. Due to the bioinspired fractal architecture, the sheet resistance of the heater can be controlled by varying the Ag nanowire loading, without sacrificing the optical transmittance. The fractal-like architecture also makes the heater flexible and shearable, so it can be used in wearable devices. The fractal-based design is also advantageous in the field of flexible electronics as this overcomes the limitations of the conventional planar designs by maximizing the surface area at the microscale, or more specifically, maximizing the surface area to volume ratio via simple scaling. The large surface area of the heater makes heat transfer to surroundings very efficient, allowing rapid response time and preventing overheating of the element. We demonstrate the potential of the bioinspired heater as a thermotherapy patch by mounting it on the surface of the skin. The insights from this study may help to repurpose fractal-like structures from nature as low-cost, high-surface-area structures for electronics applications.

RESULTS AND DISCUSSION

Fabrication and general morphology

The schematic structure of the bioinspired heater electrode and thermotherapy patch is illustrated in Fig. 1a. To fabricate the bioinspired heater electrode, the leaf skeleton of a Bodhi tree (*Ficus religiosa*) was used as a substrate. The skeleton shows fractal-like interconnections of veins at milli- and microscale. Mechanically, fractal-like architecture is responsible for high flexibility (high curvature values) and maintains the structure after repeated bending[42,43]. The leaf skeleton is mainly composed of biopolymers with lignin as the main constituent that is responsible for mechanical strength. In the first step, the leaf skeleton was soaked in the solution of $AgNO_3$ to form a seed layer of Ag ions followed by heat treatment. The presence of Ag ions on the surface was confirmed by XPS (X-Ray photoelectron spectroscopy) and the data is shown in Supplementary Fig. 1. The EDS (energy-dispersive X-ray spectroscopy) mapping was also conducted on the surface, which confirmed that the Ag is distributed throughout the surface after treatment with $AgNO_3$ (Supplementary Fig. 2). Then the leaf skeleton was placed in a hydrophobic Petri plate with different concentrations of the Ag nanowires (in ethanol + DI water, 1:1) and left to dry until the solution is completely soaked by the skeleton. The electrical resistance of the heater is dependent on the intrinsic resistance of the Ag nanowires and on the junctions between the nanowires. For stable operation, the junction resistance should be minimized. Junction resistance can be decreased by using high aspect ratio Ag nanowires[44]. The other effective way could be the conformal coating of the Ag nanowires onto the substrates, which reduce the possibility of random stacking of multiple Ag nanowires over each other. In our method, the Ag ions on the surface help in the conformal alignment of the Ag nanowires onto the surface via attractive forces between metals[45,46]. After heat treatment, Ag nanowire-coated leaf skeleton was obtained, which displayed variable sheet resistances depending on the Ag nanowire loading. The concentration of $AgNO_3$ and soaking time of the leaf skeleton in the $AgNO_3$ solution also has a minor effect on the attachment of Ag nanowires and the conductivity of the surface (refer Supplementary Table 1). The increase in the concentration of $AgNO_3$ and leaf

skeleton dipping time tends to slightly improve the conductivity of the surfaces. The 3D fractal architecture composed of lignin-based biomaterials provides support to the Ag nanowires, which formed a conductive network across the skeleton. The thermotherapy patch for the application studies was obtained by encasing the Ag nanowire-coated leaf skeleton in the transparent and biodegradable tape. The details of the fabrication procedure are provided in the "Methods" section.

The morphology of the bioinspired heater was investigated with scanning electron microscopy (SEM). Figure 1b, c shows the scanning electron micrograph of the bioinspired heater, which shows a network Ag NWs of length ~50 µm spread across the skeleton surfaces. It is also evident from the micrographs that the structure of the skeleton was preserved even after the fabrication procedure. The nanowires are evenly distributed and conformally adhered to the surface to form a continuous nano-network throughout the area. Supplementary Fig. 3 shows the bundle structure of the vascular bundles along with the peripheral interconnected fibers of the leaf skeleton. The vascular bundles along with the fibers are rich in lignin and their arrangement with fibers as fractal-like morphology provides mechanical stability and flexibility[42]. To further confirm the presence of Ag nanowires on the leaf surface, the EDS measurements were done. The corresponding EDS data are shown in Supplementary Fig. 4, which confirms the presence of Ag on the surface of the leaf skeleton.

Transmittance studies

To show the transparency of the bioinspired heater electrode, we measured the optical transmittance spectra of the leaf skeleton loaded with different concentrations of Ag nanowires. Figure 2a, b shows that the leaf skeletons with and without Ag nanowire loading display decent transparency in the regions ranging from visible to near-infrared (400–900 nm). On a flat, unstructured surface, an increase in Ag nanowire loading decreases its transparency because of the rise in the reflection of photons and stronger scattering[7]. In our case, there was no significant change in the transmittance values upon the increase in the concentration of Ag nanowires, because the nanowires are on the leaf veins and there are many holes in the surface. As evident from Fig. 2b, the relative optical transmittances of the surfaces having sheet resistances 45–8 Ω sq^{-1} were in the range of 80–86%. This indicates that even with the increase in the conductive pathways, optical transmittance is not sacrificed.

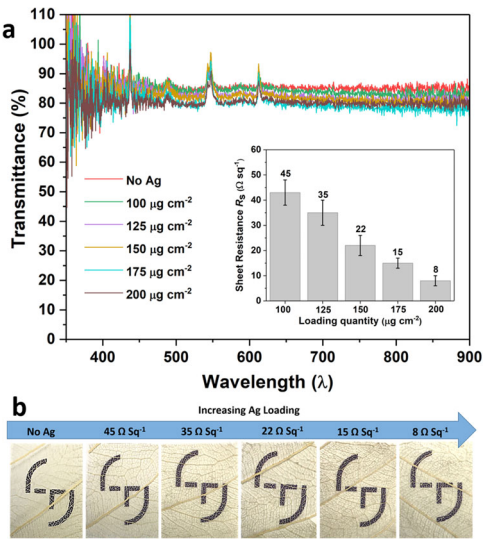

Fig. 2 Transmittance studies. a Optical transmittances of bioinspired heater electrode at different sheet resistances. Inset shows the relationship of sheet resistance at different Ag nanowire loading. Three independent measurements were done, and the error bars show the standard deviation. **b** Camera images displaying the transparency of the bioinspired heater electrode at different sheet resistances.

Heating performance

The Joule heating characteristics of the bioinspired heater are studied for the 200 µg cm^{-2} Ag nanowire density ($R_s = 8$ Ω sq^{-1}), which can be seen in Fig. 3a, b. Continuous DC voltage is applied between the two edges of the heater having dimensions of 60 mm × 60 mm and the voltage is increased by 0.5 V after every 55 s until the heater fails (Fig. 3a). It can be seen from the figure that the steady-state saturation temperature increases monotonously as the heating power is increased. At 6.5 V, the temperature surpasses 120 °C at the moment of failure. The reason may be very high local temperatures at some points at the ends (pressed for making contact with external wires), which may result in the breakage of the Ag nanowires. To show that the damage to the device is caused by temperature than the voltage, heating tests were conducted, where the heat was supplied by an external hot plate rather than the device itself. The heater was placed on a hot plate and sheet resistance was recorded at different temperatures (Supplementary Fig. 5). Above 180 °C, the resistance of the surface increased drastically, which may be due to the snapping of the Ag nanowires at this temperature[47,48]. Figure 3b shows the lowest, highest, and average temperatures across the heater along with the corresponding temperature distribution measured by the IR camera (FLIR one). Averaging over all temperatures tested, the typical variation $(T_{high} - T_{low})/T_{average}$ was ~9.0%, which shows the uniform temperature distribution across the electrode surface. The uniform temperature distribution is also evident from the corresponding IR images, which are displayed within Fig. 3a, b. A control sample without the presence of $AgNO_3$ was also fabricated. Although the nanowires attached to the surface of the skeleton, the distribution was uneven. When a bias (4.5 V) was applied to the surface, uneven distribution of the heat was clearly evident (Supplementary Fig. 6).

To check the response time and reliability of the bioinspired heater, time-dependent temperature profiles of the bioinspired heater were recorded. Figure 3c displays the time-dependent temperature profiles of heaters having different sheet resistances. For each heater, the temperature was recorded at 4.5 V. It is clear from Fig. 3c that temperature increased almost instantaneously and reached its saturation value within ~10 s. A temperature of 80 °C was reached with a heater having $R_s = 8$ Ω sq^{-1} operated at 4.5 V. To further check the response time and repeatability of the heater, the voltage driving the heater was turned on and off in quick succession. Figure 3d shows the surface temperatures of the bioinspired heater electrode at different voltages for Ag nanowire loading of 200 µg cm^{-2}. As the heterogeneity in the natural structures may lead to heterogeneity in performance, additional repeatability tests were also conducted (refer Supplementary Fig. S7). Three independent heater samples having sheet resistance ~8 Ω sq^{-1} were tested at the same bias of 4.5 V. No drastic change in the response time and the performance of the heater was observed. However, the leaf's age, size, and shape can lead to the variation in the fractal orientation and microstructures, which may lead to greater variations in the performance of the heater.

The heater displayed approximately first-order dynamics with little variation between heating/cooling cycles, higher voltages naturally corresponding to higher temperatures. The quick response can be attributed to the low thermal mass of the leaf skeleton and the high-surface area of the fractal-like geometry, even with the presence of the encapsulating tape. All forms of heat transfer—convection, conduction, and radiation—are proportional to the surface area, and fractals can have theoretically

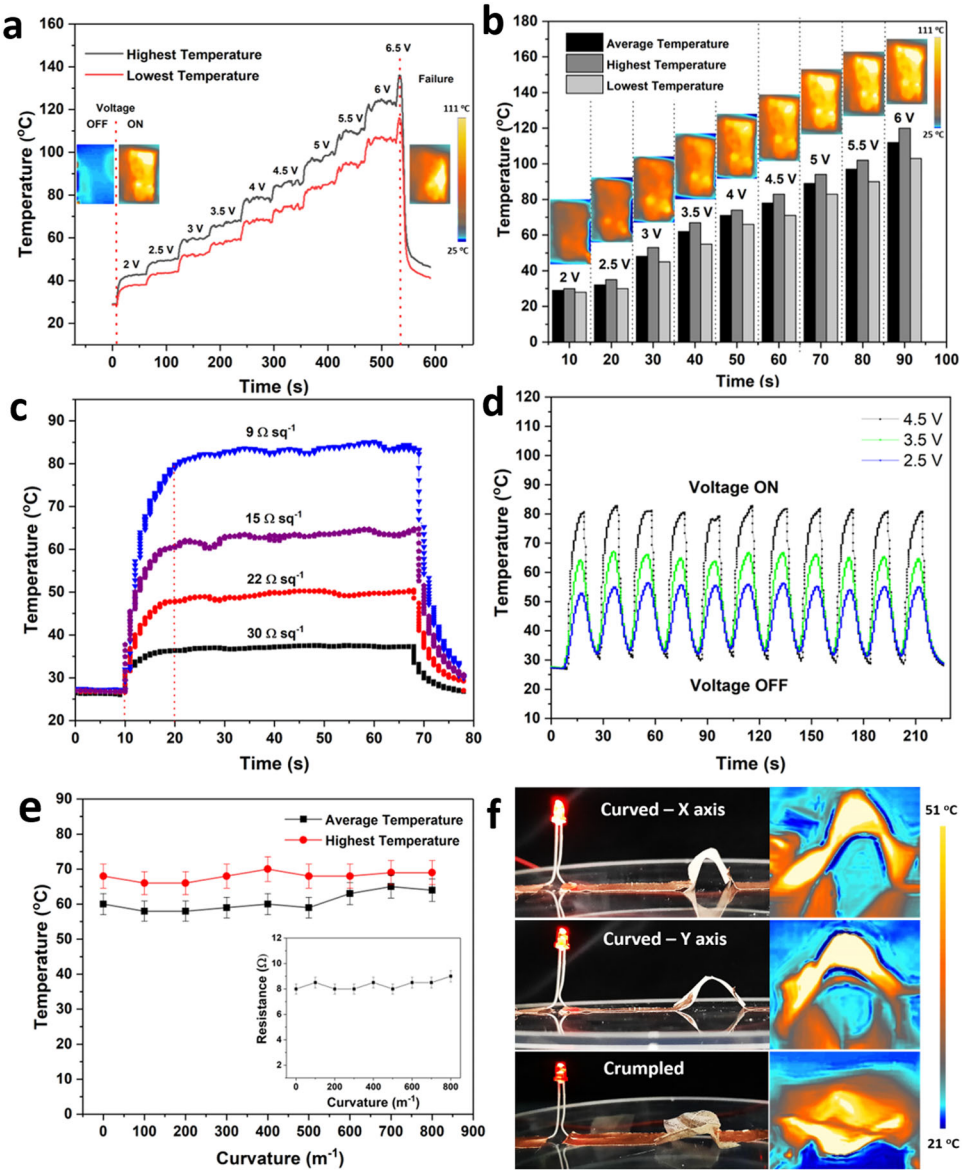

Fig. 3 Heating characteristics of the bioinspired electrode. a Transient temperature evolution of the bioinspired heater electrode at stepwise voltage rises from 2 to 6.5 V for Ag nanowire loading of 200 μg cm^{-2}. **b** Highest, lowest, and the average temperatures along with their corresponding infrared camera images. **c** Time-dependent surface temperatures with different sheet resistances at 4.5 V. **d** Temperature response over heating cycles at different voltages. **e** Change in temperature when the bioinspired heater electrode is bent. Inset shows the change in corresponding resistance values upon bending and the error bars show the standard deviations calculated from three independent measurements. **f** Digital photographs and their corresponding infrared camera images of the bioinspired heater electrode used as a conductor in the circuit when bent in the *X* axis, *Y* axis, and in crumpled positions. The Ag nanowire loading is 200 μg cm^{-2} and the bias applied is 3 V.

infinite and in practice very high-surface area for a given volume, leading to very efficient heat transfer. The basic mechanism of the heating of the surface is based on the Joule heating effect:

$$P = \frac{U^2}{R}, \tag{1}$$

where P is the heating power, U is the supplied voltage and R is the resistance of the heaters. According to the energy balance principle, this energy must be either stored as heat or transferred from the heater to its surroundings[17]:

$$\frac{U^2}{R} = c\rho V\frac{dT}{dt} + hA\,(T - T_0), \tag{2}$$

where c is specific heat capacity, ρ is the density, V is the volume of the heater, h is the heat-transfer coefficient, A is the surface area, T is the surface temperature of the electrical heater, and T_0 is the surrounding temperature. Notice that the heat-transfer coefficient here can include conduction and convection, but radiation is not considered here, as it is proportional to T^4. Nevertheless, radiation is also proportional to the surface area of the heater.

Equation (2) is a first-order linear differential equation, with a time constant $\tau = \frac{c\rho V}{hA}$. Assuming that c, ρ, and h are approximately constants, it can be seen that the response time of the heater can be made faster simply by increasing its surface to volume ratio; a property that fractal-like structures excel at. The fractal-like architecture is known to provide the optimal surface coverage, high-surface area, and minimum in-plane resistance[34,35]. Secondly, according to (2), the steady-state temperature $T_{t\to\infty} = \frac{U^2}{RhA} + T_0$. By

Table 1. Performance comparison in transparent heaters based on Ag nanowires.

S. no.	Materials	Maximum temperature (°C)	Voltage (V)	Sheet resistance (Ω sq^{-1})	Time (s)	Transmittance (%)	Biodegradable	Refs.
1	Glass/PEN	55	7	33	<200	~90	No	[18]
2	PMMA	130	1–5	0.13–1.40	10–30	44.9–85	No	[52]
3	Aramid nanofibers	260	0.5–5	0.12–390	10–30	20–90	No	[17]
4	Clay	~100	7	10	60	~90	No	[19]
5	PDMS	~200	3–10	–	~10	~70-83	No	[25]
6	PVA	~100	3–5	3.7–26	~20	74–93	Yes	[7]
7	PET	90	18	20	~10	~90	No	[53]
8	Polyimide	200	20	3–200	40	60–87	No	[32]
9	Polyimide	130	7	25	100	86	No	[16]
10	PEDOT: PSS	86	4	4	~25	70	No	[54]
11	PET	100	10	36.8	>100	76–96	No	[55]
12	Polyimide/CNT	~140	8–20	6.3–50.5	~300–600	72–97	No	[56]
13	Glass	145	~6–12	3.7–18.6	30	~82.5–90	No	[24]
14	Lignin/Leaf	~125	6	8–45	5	80–86	Yes	This work

increasing the surface area, the steady-state temperature for a giving heating power is decreased, meaning that the risk of overheating the heating element is reduced. Taken together, these two aspects explain the rationale why fractal-like biotic structures with high-surface area to volume ratio lead to more efficient heaters.

To demonstrate the flexibility of these bioinspired heaters, the resistance, and temperature when operated at a constant voltage were recorded while the heater was bent, as shown in Fig. 3e. The curvature of the heater surface was estimated from photographs. The temperature of the surface does not change much as the electrode is subject to bending. For the experiment, the electrode with Ag nanowire loading of 200 μg cm^{-2} and sheet resistance of 8 Ω sq^{-1} was used and a fixed voltage of 3.5 V was applied. When the curvature is increased from 0 to 800 m^{-1}, the average temperature recorded was ~61 °C with a relative standard deviation of only 4.3 %. The average sheet resistance also does not change much, displaying the RSD of ~4.0%, which can be seen in the inset of Fig. 3e. The reason for variation in the temperature and resistance values during the bending of the electrode could be due to the increased contacts between the Ag nanowires[49]. It is noteworthy to mention that the leaf skeletons are not perfectly isotropic in-plane, hence these may show different flexibility and change in resistance depending on the direction of bending. This is in contrast with microfabricated fractal-inspired structures[50], where the design can be carefully controlled and thus can be made more isotropic. To check if the anisotropicity of the leaf skeleton affects its heating, we bent the heater in the *X* and *Y* axis and even crumpled the surface. As evident from Fig. 3f, the resistivity of the heater is largely independent of the bending and its direction, and the heating performance is not significantly affected by the bending (Fig. 3f, insets). To test how the bioinspired heater ages, the heating experiment was conducted after storing the heater in ambient conditions for 1 month. The SEM images of a 1-month-old heater are shown in Supplementary Fig. 8 where intact Ag nanowires can be seen covering the whole surface. The time-dependent surface temperature profile of a 1-month-old heater is shown in Supplementary Fig. 9. From the figure, it is evident that there is no drastic change in the performance of the heater. However, a decrease in the operating temperature is observed, which may be due to oxidation of the Ag nanowires; oxidation can be prevented or reduced by proper encapsulation[51].

Table 1 compares our results to recently reported film heaters based on Ag nanowires including material and fabrication procedure, sheet resistances, nanowire loading quantity, operating voltage, minimum time to reach operating temperature (response time), and their applications. In view of the studies reported in the literature, we conclude that our proposed bioinspired heaters based on leaf skeletons and Ag nanowires have a very rapid response time in and low sheet resistances without compromising transmittance compared to other Ag-based film heaters. It is noteworthy to mention that for applications that require large surface areas, the scalability of the heater is important: how large heaters can be fabricated and at what cost. The leaf puts a natural boundary on how large the heater can be. So, if a larger heater area is needed, multiple heaters can be used in parallel or series. The fabrication procedure is facile and is not limited to the area restrictions provided by the conventional fabrication equipment, hence scale-up is easy if we have a large area.

Application as a thermotherapy patch

Applications of the bioinspired heater electrode in wearable thermotherapy have been demonstrated. The thermotherapy patch was fabricated just by encasing the heater electrode in a biodegradable transparent tape (3 M). As the tape is flexible and light, the bioinspired heater can be simply mounted on any surface with very good conformal coverage. The tape is also biocompatible and does not irritate the skin. The bioinspired thermotherapy patch is affixed on the different locations on the human body such as the wrist, cubital fossa area, and elbow, in order to test the versatility during bending and twisting, which are commonly involved in normal human activities. The temperature of the bioinspired thermotherapy patch was elevated in the range of 45–50 °C by applying a voltage of 3 V. Apart from the voltage, the Ag nanowire loading can also be used to control the overheating. This range of temperature is suitable for use in wearable devices, which are used to relieve pain and stiffness. Figure 4a shows the digital camera images and their representative temperature profiles of the thermotherapy patch mounted on the wrist during the neutral, inward bending, and outward bending. Figure 4b, c shows the temperature profiles of the bioinspired thermotherapy patch affixed to the cubital fossa and elbow respectively during the bending conditions. It is clear from the images that the bioinspired thermotherapy patch provides uniform heating and good performance at mechanical disturbances occurring during normal human activities, while still transparent enough to see through. The bioinspired heater surface can also be used in heating water at low voltage as demonstrated in Supplementary Fig. 10.

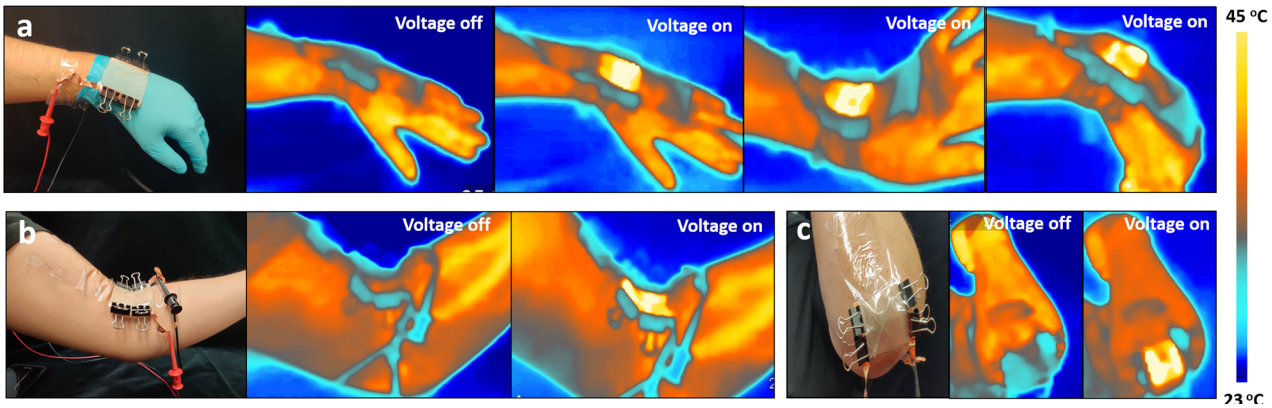

Fig. 4 Digital and infrared photographs of the thermotherapy patch in use. a Temperature distribution image of bioinspired thermotherapy patch affixed to the human wrist in normal, inward, and outward bending conditions. **b**, **c** The patch affixed to the cubital fossa area and elbow, respectively.

As the main constituent of the heater electrode and the encapsulating tape is cellulose, it can be considered as biodegradable[57]. In literature, it has been demonstrated that the leaf skeletons when stored in tap water show significant biodegradation within a few days[58]. In addition, Ag nanowire can be readily degradable using UV irradiation and heat treatment[59]. Ag itself is not toxic to the environment and environmental species and it has been found that the bioaccumulation of the Ag leads to biologically nonreactive compounds during biological processes[60].

In conclusion, we fabricated a flexible, transparent, and fast response time bioinspired heater using leaf skeletons and Ag nanowires. The properties of the heater are attributed to the fractal-like geometry of the leaf skeleton. The fabrication process, microstructures, transparency, thermal, and mechanical properties of the bioinspired heater electrodes were investigated in detail. The Ag nanowires conformally attach to the fractal-like structures due to the Ag ion coating on the surface. The high-surface area results in efficient heating at a very rapid response time (~5 s). Such response time to our knowledge is best among the Ag nanowire-based transparent film heaters. The application of the heater was demonstrated in the fabrication of ultra-flexible and transparent thermotherapy patch. As the bioinspired thermotherapy patch is entirely made of plant-based materials, it may help to reduce the carbon footprint and electronic waste. The overall materials used in the fabrication of bioinspired thermotherapy patch are eco-friendly, economical, easily accessible, and easy to fabricate compared to the other transparent heaters that require complex and expensive fabrication procedures. One shortcoming of our bioinspired heater is the lack of stretchability. This may be improved by replicating the fractal structures using biocompatible polymers that have intrinsic stretchability. In the future, we hope to extend this work towards stretchable designs, by utilizing the unexplored natural biotic and kirigami inspired architectures. In short, our study shows that fractal-like geometries for flexible electronics can be easily fabricated by reusing and repurposing fractal-like substrates from nature, instead of using traditional cleanroom micro-/nanofabrication methods that may be slow and costly.

METHODS

Materials

For the fabrication of the leaf skeleton electrode, the leaf skeleton of *Ficus religiosa* was purchased from '*Skeleton Leaf - Just the Leaves*', United Kingdom. $AgNO_3$, Ag nanowires for the fabrication of heater electrode, 1H,1H,2H,2H-perfluorodecyltriethoxysilane, were purchased from Merck, Finland. All the chemicals were used as received. For the fabrication of the thermotherapy patch, biodegradable tape (for encasing the heater surface) was purchased from 3M.

Fabrication of bioinspired heater surface and thermotherapy patch

In the first step of the fabrication, Petri plates were made hydrophobic. The Petri plates were first scored with sandpaper and were placed inside a desiccator for 15 min along with 1H,1H,2H,2H-perfluorodecyltriethoxysilane, followed by heat treatment inside the oven for 100 °C. The leaf skeletons were dipped in 5 mM solution of $AgNO_3$ in DI water (ELGA purelab) for the 30 s and dried at room temperature. In the next step, the leaf skeletons were placed inside the Petri dishes along with the different concentrations of Ag nanowire (100–200 μg cm^{-2}, diluted in ethanol + DI water, 1:1), and allowed to dry under ambient conditions. This makes sure that the leaf skeleton having an $AgNO_3$ layer adsorbs all the nanowire solution put inside the Petri plates. In the final step, the skeletons were placed over a hot plate (maximum temperature of 120 °C) and allowed to dry for 1 h. Copper tape (3 M) was applied at the edges of the Ag nanowire-coated surfaces to make conductive contacts. The copper tapes were pressed with the paper clips to keep the contacts uniform. For the fabrication of the thermotherapy patch, the skeleton coated with Ag nanowire was encased with biodegradable transparent tape on both sides.

Characterization

High-resolution surface structure characterization was performed using an SEM (scanning electron microscope) (Jeol IT-500) operating at 5 kV. Elemental analysis was done using an EDS (Energy-dispersive X-ray spectroscopy) attachment linked to SEM (JEOL). The infrared images were captured using the FLIR One Pro infrared camera. The sheet resistance of the surfaces was measured using an LCR meter. The surface composition was measured utilizing X-ray photoelectron spectroscopy (XPS) employing a non-monochromatized X-ray source (AlKα, 1486.6 eV) and VG Microtech CLAM 4 hemispherical electron spectrometer. The binding energy scale was calibrated according to C 1s C–C/H peak at 284.8 eV. The background-subtracted XPS peaks were least-squares fitted with symmetrical mixed Gaussian–Lorentzian component line shapes.

DATA AVAILABILITY

The data generated and analyzed during the study are available from the corresponding authors on a reasonable request.

Received: 16 April 2020; Accepted: 28 September 2020;
Published online: 15 October 2020

REFERENCES

1. Li, Z. et al. Transparent electrothermal film defoggers and anti-icing coatings based on wrinkled graphene. *Small* **16**, 1905945 (2020).
2. Lee, D., Bang, G., Byun, M. & Choi, D. Highly flexible, transparent and conductive ultrathin silver film heaters for wearable electronics applications. *Thin Solid Films* **697**, 137835 (2020).

3. Kim, D. et al. Transparent flexible heater based on hybrid of carbon nanotubes and silver nanowires. *Carbon N. Y.* **63**, 530–536 (2013).
4. Gupta, R., Rao, K. D. M., Kiruthika, S. & Kulkarni, G. U. Visibly transparent heaters. *ACS Appl. Mater. Interfaces* **8**, 12559–12575 (2016).
5. Zhang, M. et al. Weft-Knitted fabric for a highly stretchable and low-voltage wearable heater. *Adv. Electron. Mater.* **3**, 1700193 (2017).
6. Choi, S. et al. Stretchable heater using ligand-exchanged silver nanowire nanocomposite for wearable articular thermotherapy. *ACS Nano* **9**, 6626–6633 (2015).
7. Lan, W. et al. Ultraflexible transparent film heater made of Ag nanowire/PVA composite for rapid-response thermotherapy pads. *ACS Appl. Mater. Interfaces* **9**, 6644–6651 (2017).
8. Wang, T. et al. Flexible transparent electronic gas sensors. *Small* **12**, 3748–3756 (2016).
9. Liu, P., Liu, L., Jiang, K. & Fan, S. Carbon-nanotube-film microheater on a polyethylene terephthalate substrate and its application in thermochromic displays. *Small* **7**, 732–736 (2011).
10. Sun, K., Yamaguchi, A., Ishida, Y., Matsuo, S. & Misawa, H. A heater-integrated transparent microchannel chip for continuous-flow PCR. *Sens. Actuators B Chem.* **84**, 283–289 (2002).
11. Suh, M., Curto, S., Prakash, P. & van Rhoon, G. in *Wearable Bioelectronics* 179–200 (Elsevier, 2020).
12. Welch, V. et al. Thermotherapy for treating rheumatoid arthritis. *Cochrane Database Syst. Rev.* **1**, CD002826 (2002).
13. Gaudreault, Y., Lebeau, M. & Robitaille, R. Thermotherapeutic pad. U.S. Patent 5,300,104. (1994).
14. Guibert, R. & Guibert, B. Universal thermotherapy applicator. U.S. Patent 5,190,031 (1993).
15. Kim, H. et al. Highly stretchable and wearable thermotherapy pad with micropatterned thermochromic display based on Ag nanowire–single-walled carbon nanotube composite. *Adv. Funct. Mater.* **29**, 1901061 (2019).
16. Lu, H.-Y., Chou, C.-Y., Wu, J.-H., Lin, J.-J. & Liou, G.-S. Highly transparent and flexible polyimide–AgNW hybrid electrodes with excellent thermal stability for electrochromic applications and defogging devices. *J. Mater. Chem. C* **3**, 3629–3635 (2015).
17. Ma, Z. et al. High-performance and rapid-response electrical heaters based on ultraflexible, heat-resistant, and mechanically strong aramid nanofiber/Ag nanowire nanocomposite papers. *ACS Nano* **13**, 7578–7590 (2019).
18. Celle, C. et al. Highly flexible transparent film heaters based on random networks of silver nanowires. *Nano Res.* **5**, 427–433 (2012).
19. Kim, T. et al. Uniformly interconnected silver-nanowire networks for transparent film heaters. *Adv. Funct. Mater.* **23**, 1250–1255 (2013).
20. Lee, S. J. et al. SWCNT–Ag nanowire composite for transparent stretchable film heater with enhanced electrical stability. *J. Mater. Sci.* **53**, 12284–12294 (2018).
21. Kang, J. et al. High-performance graphene-based transparent flexible heaters. *Nano Lett.* **11**, 5154–5158 (2011).
22. Lee, P. et al. Highly stretchable or transparent conductor fabrication by a hierarchical multiscale hybrid nanocomposite. *Adv. Funct. Mater.* **24**, 5671–5678 (2014).
23. Cheong, H.-G., Song, D.-W. & Park, J.-W. Transparent film heaters with highly enhanced thermal efficiency using silver nanowires and metal/metal-oxide blankets. *Microelectron. Eng.* **146**, 11–18 (2015).
24. Huang, Y. et al. Self-limited nanosoldering of silver nanowires for high-performance flexible transparent heaters. *ACS Appl. Mater. Interfaces* **11**, 21850–21858 (2019).
25. Hong, S. et al. Highly stretchable and transparent metal nanowire heater for wearable electronics applications. *Adv. Mater.* **27**, 4744–4751 (2015).
26. Gupta, R. et al. Spray coating of crack templates for the fabrication of transparent conductors and heaters on flat and curved surfaces. *ACS Appl. Mater. Interfaces* **6**, 13688–13696 (2014).
27. Kwon, N., Kim, K., Heo, J., Yi, I. & Chung, I. Study on Ag mesh/conductive oxide hybrid transparent electrode for film heaters. *Nanotechnology* **25**, 265702 (2014).
28. Jia, L.-C. et al. Highly efficient and reliable transparent electromagnetic interference shielding film. *ACS Appl. Mater. Interfaces* **10**, 11941–11949 (2018).
29. Chen, J. et al. Enhanced oxidation-resistant Cu–Ni core–shell nanowires: controllable one-pot synthesis and solution processing to transparent flexible heaters. *Nanoscale* **7**, 16874–16879 (2015).
30. Hsu, P.-C. et al. Personal thermal management by metallic nanowire-coated textile. *Nano Lett.* **15**, 365–371 (2015).
31. Hsu, P.-C. et al. Performance enhancement of metal nanowire transparent conducting electrodes by mesoscale metal wires. *Nat. Commun.* **4**, 2522 (2013).
32. Pyo, K. & Kim, J.-W. Transparent and mechanically robust flexible heater based on compositing of Ag nanowires and conductive polymer. *Compos. Sci. Technol.* **133**, 7–14 (2016).
33. Liu, Y., He, K., Chen, G., Leow, W. R. & Chen, X. Nature-inspired structural materials for flexible electronic devices. *Chem. Rev.* **117**, 12893–12941 (2017).
34. Han, B. et al. Optimization of hierarchical structure and nanoscale-enabled plasmonic refraction for window electrodes in photovoltaics. *Nat. Commun.* **7**, 1–8 (2016).
35. James, S. & Contractor, R. Study on nature-inspired fractal design-based flexible counter electrodes for dye-sensitized solar cells fabricated using additive manufacturing. *Sci. Rep.* **8**, 17032 (2018).
36. Werner, D. H., Haupt, R. L. & Werner, P. L. Fractal antenna engineering: The theory and design of fractal antenna arrays. *IEEE Antennas Propag. Mag.* **41**, 37–58 (1999).
37. Díaz-Lantada, A., Mosquera, A., Endrino, J. L. & Lafont, P. Design and rapid prototyping of DLC coated fractal surfaces for tissue engineering applications. in. *J. Phys. Conf. Ser.* **252**, 12003 (2010).
38. Han, B. et al. Bio-inspired networks for optoelectronic applications. *Nat. Commun.* **5**, 5674 (2014).
39. Chen, Y. & Cheng, P. Heat transfer and pressure drop in fractal tree-like microchannel nets. *Int. J. Heat. Mass Transf.* **45**, 2643–2648 (2002).
40. Orbach, R. Dynamics of fractal networks. *Science* **231**, 814–819 (1986).
41. Thekkekara, L. V. & Gu, M. Bioinspired fractal electrodes for solar energy storages. *Sci. Rep.* **7**, 45585 (2017).
42. Schnepp, Z., Yang, W., Antonietti, M. & Giordano, C. Biotemplating of metal carbide microstructures: the magnetic leaf. *Angew. Chem. Int. Ed.* **49**, 6564–6566 (2010).
43. Beck, C. B. *An Introduction to Plant Structure and Development: Plant Anatomy for the Twenty-First Century* (Cambridge University Press, 2010).
44. Bellew, A. T., Manning, H. G., Gomes da Rocha, C., Ferreira, M. S. & Boland, J. J. Resistance of single Ag nanowire junctions and their role in the conductivity of nanowire networks. *ACS Nano* **9**, 11422–11429 (2015).
45. Heine, V. & Marks, L. D. Competition between pairwise and multi-atom forces at noble metal surfaces. *Surf. Sci.* **165**, 65–82 (1986).
46. Rehr, J. J., Zaremba, E. & Kohn, W. van der Waals forces in the noble metals. *Phys. Rev. B* **12**, 2062 (1975).
47. Fan, Y. J. et al. Highly robust, transparent, and breathable epidermal electrode. *ACS Nano* **12**, 9326–9332 (2018).
48. Peng, P. et al. Room-temperature pressureless bonding with silver nanowire paste: towards organic electronic and heat-sensitive functional devices packaging. *J. Mater. Chem.* **22**, 12997–13001 (2012).
49. Lee, P. et al. Highly stretchable and highly conductive metal electrode by very long metal nanowire percolation network. *Adv. Mater.* **24**, 3326–3332 (2012).
50. Fan, J. A. et al. Fractal design concepts for stretchable electronics. *Nat. Commun.* **5**, 3266 (2014).
51. Elechiguerra, J. L. et al. Corrosion at the nanoscale: the case of silver nanowires and nanoparticles. *Chem. Mater.* **17**, 6042–6052 (2005).
52. He, X. et al. Temperature-controlled transparent-film heater based on silver nanowire–PMMA composite film. *Nanotechnology* **27**, 475709 (2016).
53. Cai, Y. et al. A facile method to prepare silver nanowire transparent conductive film for heaters. *Mater. Lett.* **249**, 66–69 (2019).
54. Ji, S., He, W., Wang, K., Ran, Y. & Ye, C. Thermal response of transparent silver nanowire/PEDOT: PSS film heaters. *Small* **10**, 4951–4960 (2014).
55. Seok, H.-J., Kim, J.-K. & Kim, H.-K. Effective passivation of Ag nanowire network by transparent tetrahedral amorphous carbon film for flexible and transparent thin film heaters. *Sci. Rep.* **8**, 13521 (2018).
56. Goak, J. C. et al. Stable heating performance of carbon nanotube/silver nanowire transparent heaters. *Appl. Surf. Sci.* **510**, 145445 (2020).
57. Simon, J., Müller, H. P., Koch, R. & Müller, V. Thermoplastic and biodegradable polymers of cellulose. *Polym. Degrad. Stab.* **59**, 107–115 (1998).
58. Elsayes, A. et al. Plant-based biodegradable capacitive tactile pressure sensor using flexible and transparent leaf skeletons as electrodes and flower petal as dielectric layer. *Adv. Sustain. Syst.* **4**, 2000056 (2020).
59. Choo, D. C. & Kim, T. W. Degradation mechanisms of silver nanowire electrodes under ultraviolet irradiation and heat treatment. *Sci. Rep.* **7**, 1696 (2017).
60. Ratte, H. T. Bioaccumulation and toxicity of silver compounds: a review. *Environ. Toxicol. Chem.* **18**, 89–108 (1999).

ACKNOWLEDGEMENTS

This work was supported by the Academy of Finland (Grants: #299087 and #292477). We are grateful for the support from the Tampere Microscopy Centre for the characterization of the surfaces.

AUTHOR CONTRIBUTIONS

V. Sharma and V. Sariola conceived the idea. V. Sharma designed the project, experiments, and wrote the manuscript. A.K. conducted transmittance studies. K.Y. helped in the general experiments. K.L. conducted the XPS measurements. All authors reviewed the manuscript.

COMPETING INTERESTS

The authors declare no competing interests.

ADDITIONAL INFORMATION

Supplementary information is available for this paper at https://doi.org/10.1038/s41528-020-00091-8.

Correspondence and requests for materials should be addressed to V.S. or V.S.

Reprints and permission information is available at http://www.nature.com/reprints

Publisher's note Springer Nature remains neutral with regard to jurisdictional claims in published maps and institutional affiliations.